

**KERNFORSCHUNGSZENTRUM**

**KARLSRUHE**

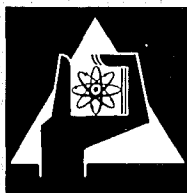
Dezember 1973

KFK 2013

Institut für Angewandte Kernphysik

**Analysis of Thin Evaporated und Sputtered Superconducting  
Films by the Backscattering Technique**

M. Gettings, B. Kraeft, G. Linker, O. Meyer



**GESELLSCHAFT FÜR KERNFORSCHUNG M. B. H.  
KARLSRUHE**



## BACK-SCATTERING ENERGY LOSS PARAMETER MEASUREMENTS IN THIN METAL FILMS\*

G. LINKER, O. MEYER AND M. GETTINGS

*Institut für Angewandte Kernphysik, Kernforschungszentrum, Karlsruhe (Germany)*

(Received August 10, 1973)

The back-scattering energy loss parameter  $[S]$  has been determined directly from evaporated metal layers of Ti, V, Ni, Mo and Ta for 2.0 MeV  $\text{He}^+$  ions and a back-scattering angle  $\theta = 168^\circ$ . Reasonable agreement has been found with  $[S]$  values calculated from experimental  $dE/dx$  results tabulated by Ziegler and Chu. Discrepancies in  $[S]$  values occurred for thin Mo and Ta layers ( $< 500 \text{ \AA}$ ) and for Ti and V layers evaporated in a poor vacuum. Variations are thought to be due to film growth effects and impurity incorporation during deposition. A correlation of  $[S]$  values with layer superconducting properties has been observed.

---

### 1. INTRODUCTION

The back-scattering of light ions from solid targets has become an important technique in the analysis of surfaces and layers over a depth range of about 300 to 10000  $\text{Å}$ <sup>1,2</sup>. In the analysis of the energy spectra produced by the back-scattered ions, an important factor is the back-scattering energy loss parameter  $[S]$ . This parameter enables the energy scale of such spectra to be converted directly into a depth scale and is used for the determination of mass concentrations. The  $[S]$  value for a given target-ion system can be calculated from a knowledge of the atomic stopping cross section  $\epsilon$  as a function of the ion energy. Discrepancies in this relationship between the stopping cross section and the energy still exist however, and can lead to variations in determined  $[S]$  values.

In this present study experimental  $[S]$  values are presented for the transition metals Ti, V, Ni, Mo and Ta from back-scattered energy spectra obtained from layers of known thicknesses. While the method gives  $[S]$  values for a fixed laboratory back-scattering angle it requires no knowledge of stopping cross section-energy relationships.

A further advantage of the technique is that the influence of layer properties on  $[S]$  values can be investigated. Such variations in properties arise during the growth of thin films, especially when intermediate stages follow the nucleation

---

\* Paper presented at the International Conference on Ion Beam Surface Layer Analysis, Yorktown Heights, New York, U.S.A., June 18–20, 1973.

and precede the formation of continuous layers. Such effects have been observed, using the back-scattering technique, during the growth of Sn films<sup>3</sup>. Changes in layer properties, for example by impurity incorporation or by structural changes, can be produced during deposition. Variation in  $[S]$  values for such layers reflect changes in the physical properties such as the superconducting transition temperature and transition width.

Experimental  $[S]$  values obtained in this study are compared with values calculated from the latest available theoretical and experimental stopping cross sections, as tabulated by Ziegler and Chu<sup>4</sup>.

## 2. EXPERIMENTAL

Layers of Ti, V, Ni, Mo and Ta of different thicknesses were prepared by electron-gun evaporation onto single-crystal quartz substrates in ultrahigh vacuum; a pressure of  $1 \times 10^{-8}$  to  $5 \times 10^{-8}$  torr was maintained during evaporation. In addition, layers of Ti and V were evaporated by resistance heating in another vacuum system, over a pressure range of  $2 \times 10^{-5}$  to  $8 \times 10^{-6}$  torr. The distance separating source and substrate in both evaporation chambers was about 15 cm, so that layers of uniform thickness were obtained.

Layer thicknesses were measured with a stylus instrument, which relies on the movement of a stylus over a changing surface topography, vertical fluctuations being amplified by a maximum factor of  $10^6$ . This amplification means that steps in the trace of the stylus could be measured with a resolution of  $\pm 50 \text{ \AA}$ . Layer thicknesses were measured as the difference in the step height between the substrate and the layer levels.

Back-scattering energy spectra were obtained by the wide angle scattering ( $168^\circ$ ) of 2.0 MeV  $^4\text{He}^+$  ions supplied by a 3 MeV Van de Graaff accelerator. An accurate assessment of the ion energy was achieved by using a  $^{241}\text{Am}$   $\alpha$ -particle source and the  $\text{He}^+$  ion back-scattering from a gold film. The energy of the detected particles was corrected for the energy loss in the gold film of the surface barrier detector. The final calibrated energy was calculated to be 2.008 MeV and this energy was reproducible by using a Li resonance to fix the field of the analysing magnet. The channel-to-energy conversion of the system, which was determined from a calibration sample consisting of thin evaporated gold and aluminium films on a graphite substrate, was calculated to be 3.35 keV/channel.

Collimated  $\text{He}^+$  ion beams impinged at normal incidence on the surface of the metal layers and the back-scattered fraction of the ions was detected by a silicon surface barrier detector having a resolution of 16 keV. Beam currents were held constant at a value of 10 nA and secondary electrons were suppressed using a negatively biased Faraday grid. Back-scattered energy spectra were taken near to the substrate-metal layer edge and in the region of the thickness measurement.

## 3. ANALYSIS

The experimental  $[S]$  values presented in this study were obtained from the ratio of the observed energy loss in the metal layer to the layer thickness. The

energy difference  $\Delta E$  (in eV) between particles scattered from the front and rear surfaces of the films was calculated from the layer full width at half maximum (FWHM) as measured in channels and the known value of the channel-to-energy conversion. The  $\Delta E$  value used here was corrected for peak broadening produced by the finite detector resolution. In Fig. 1, a typical back-scattering spectrum from a Mo layer on a quartz substrate is presented, illustrating characteristic results for both thickness and back-scattering measurements.

The  $[S]$  values were then calculated from the simple formula

$$[S] = \frac{\Delta E}{X} \text{ eV/\AA} \tag{1}$$

where  $\Delta E$  is the energy difference in electron volts and  $X$  is the layer thickness in angstroms. For each of the different elements, layers of various thicknesses were analysed and an arithmetic mean of the values obtained from each element was taken as the result for the  $[S]$  value.

In addition,  $\Delta E$  should be a linear function of  $X$  for layers of the same metal and thus from the measured values the coefficients for a straight line  $\Delta E = aX + b$  were determined by a least-squares fit, the slope of this line giving the  $[S]$  value directly and the error in  $[S]$  being obtained from the least-squares procedure. Discrepancies between the mean  $[S]$  values and those determined from the slope  $a$ , together with the deviations from zero of the intercept  $b$  on the  $y$ -axis, are a measure of the spread of the single  $[S]$  values determined for different layers of a particular element.

The  $[S]$  value as a function of the stopping cross section  $dE/dx$  has been defined<sup>5</sup> by the following equation:

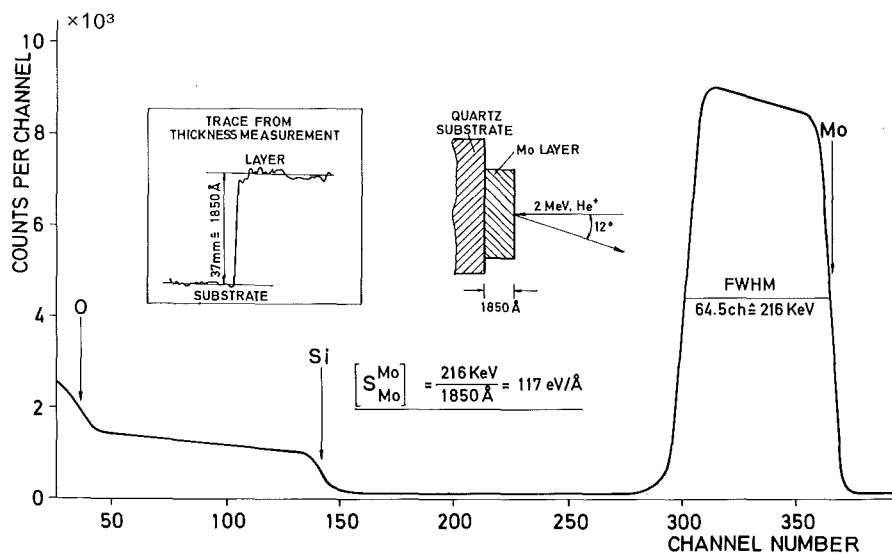


Fig. 1. A typical back-scattering spectrum from a Mo layer grown on a quartz substrate. A trace from a stylus instrument for a thickness measurement of this layer is included, together with a diagrammatic representation of the layer-beam system.

$$[S] = \alpha \left. \frac{dE}{dx} \right|_{E_1} - \frac{1}{\cos \theta} \left. \frac{dE}{dx} \right|_{\alpha E_1} \quad (2)$$

where  $\alpha$  is the fractional energy loss due to surface scattering,  $\theta$  is the scattering angle in the laboratory system,  $E_1$  is the energy of the incident particles and  $dE/dx$  is the energy loss at energies  $E_1$  and  $\alpha E_1$ . This equation was used for the evaluation of both theoretical and experimental  $[S]$  values from the calculated and measured  $dE/dx$  values tabulated by Ziegler and Chu<sup>4</sup> and is valid for layers in which the dependence of  $dE/dx$  on energy can be neglected.

#### 4. RESULTS AND DISCUSSION

The results for the  $[S]$  values presented in this study are valid for an incident energy of  $\text{He}^+$  ions of 2.0 MeV and for a fixed back-scattering angle  $\theta = 168^\circ$ .

Energy losses for Ti, V and Ni layers are plotted against layer thickness in Fig. 2, together with the straight lines and their equations obtained from a least-squares fit. The linear dependence of  $\Delta E$  on layer thickness up to thicknesses of about 4000 Å indicates that eqn. (2) is applicable for these thicknesses for the metals investigated. It is considered that the most accurate results are for those metals whose straight lines approach closest to the origin, *i.e.* Ni and V. Values obtained from the slope for these elements show the smallest calculated error and are in good agreement with the mean values. This agreement is demonstrated in Table I, where  $[S]$  values obtained from the layers prepared in ultrahigh vacuum are compared with the calculated values from the experimental and theoretical data supplied by Ziegler and Chu<sup>4</sup>. Bulk densities have been assumed for these layers as back-scattering yields were compatible with yields from bulk samples.

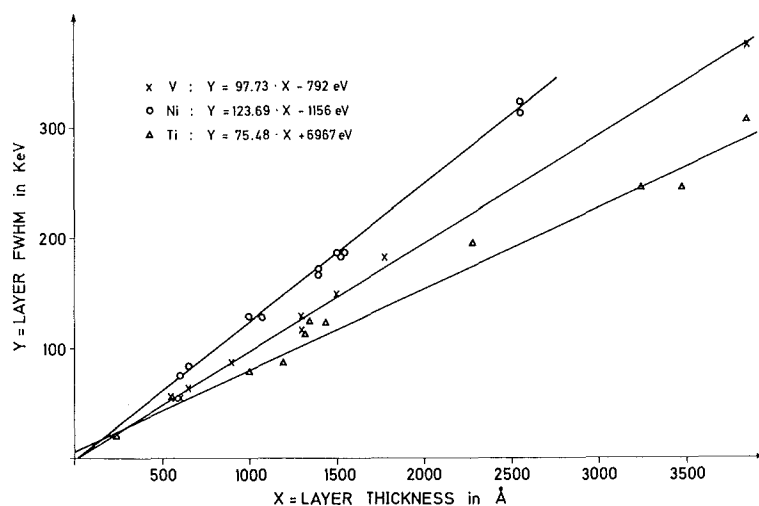


Fig. 2. Layer FWHM measurement in keV plotted as a function of layer thickness for V, Ni and Ti, together with the straight lines and their equations from a least-squares fit through the measurement points.

In general, for the metal systems investigated, agreement between our values and the experimental values from Ziegler and Chu is good. Discrepancies between our mean values and those obtained from the slope  $a$ , especially for Ti and Ta, are due to the scatter of the  $[S]$  values obtained from individual layers. In some cases we believe that this scatter is due to difficulties in layer thickness determination.

TABLE I

$[S]$  VALUES, FROM THE PRESENT WORK, DETERMINED AS MEAN VALUES AND FROM THE SLOPE OF A LINE PRODUCED FROM A LEAST-SQUARES FIT ARE COMPARED WITH THOSE CALCULATED FROM THEORETICAL AND EXPERIMENTAL  $dE/dx$  VALUES TABULATED BY ZIEGLER AND CHU<sup>4</sup>

Element	$[S]$ values for 2 MeV $^4\text{He}^+$ ions, $\theta = 168^\circ$			
	Calculated from $dE/dx$ values as tabulated by Ziegler and Chu		Present work	
	Theoretical	Experimental	Value from slope	Mean value
Ti	74.9	79.1	$75.5 \pm 2.9$	81.5
V	92.4	94.9	$97.7 \pm 1.9$	96.4
Ni	110.8	119.0	$123.7 \pm 2.3$	123.1
Mo	110.3	118.7	$122.1 \pm 4.6$	118.7
Ta	109.4	115.3	$125.7 \pm 10.3$	115.0

Characteristic variations in  $[S]$  for a particular metal were observed when layer growth conditions were altered. For example, for thin layers ( $< 500 \text{ \AA}$ ) of Mo and Ta consistently smaller  $[S]$  values were measured. Values of  $81.2 \text{ eV/\AA}$  (Mo) and  $83 \text{ eV/\AA}$  (Ta) were obtained for such layers, compared with  $118.7 \text{ eV/\AA}$  (Mo) and  $115 \text{ eV/\AA}$  (Ta) for thick layers. These discrepancies may have a number of causes, such as inhomogeneous layer growth resulting in a reduced layer density, enhanced impurity incorporation in thin layers or the influence of substrate roughness on layer topography. While errors in thickness measurements for thin layers were greater, consistently low  $[S]$  values were still obtained in the Mo and Ta layers studied.

For Ti and V layers evaporated in a vacuum of about  $10^{-5}$  torr, reduced  $[S]$  values were again observed. These reduced values are plotted as a function of layer thickness in Fig. 3, together with the level for the mean  $[S]$  value obtained from layers evaporated in a vacuum of about  $10^{-8}$  torr. The over-all reduction in  $[S]$  values is thought to be produced by the pronounced gettering effect of both Ti and V during evaporation. This well-known gettering was observed here by an improvement of the vacuum in the chamber during evaporation. As impurity incorporation decreased with increasing evaporation time (layer thickness), the deviation in  $[S]$  from the ultrahigh vacuum value was reduced. This deviation in  $[S]$  is most pronounced for Ti, while for V the process is governed by the limited solubility of impurities, resulting in a weaker dependence of  $[S]$  on thickness.

The influence of impurity incorporation can be readily seen in back-scattering spectra from layers grown in a poor vacuum. A typical example is shown in Fig. 4, which compares V layers evaporated onto quartz substrates at pressures of about  $10^{-5}$  and  $10^{-8}$  torr. From these spectra it is apparent that the main impurity

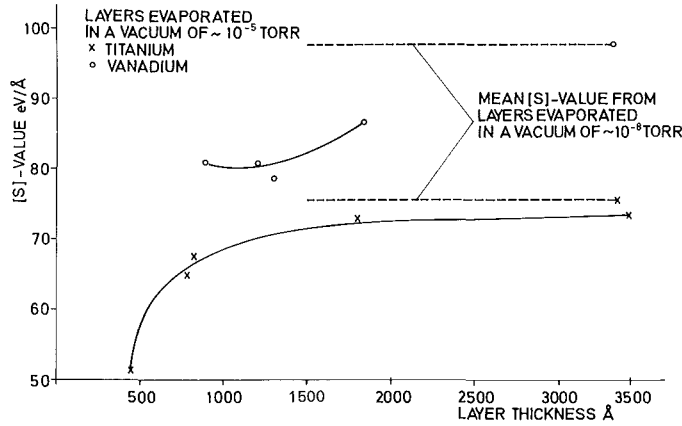


Fig. 3. Variation of the [S] values determined for Ti and V layers evaporated in a vacuum of  $10^{-5}$  torr as a function of layer thickness. Also included are the levels for the mean [S] values obtained from layers evaporated in a vacuum of  $10^{-8}$  torr.

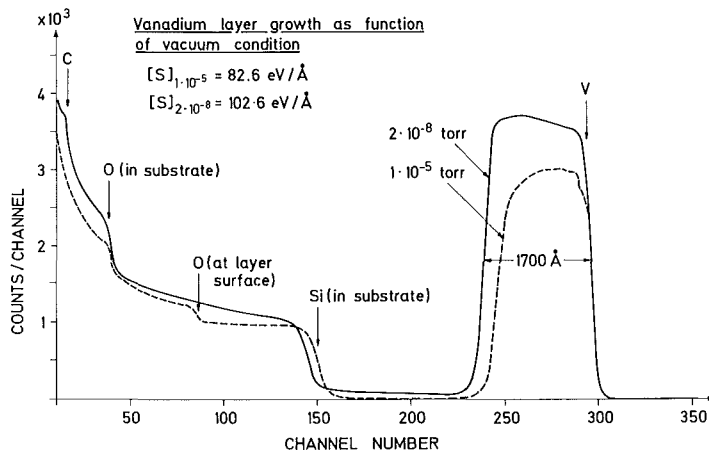


Fig. 4. Back-scattering spectra of V layers evaporated onto quartz substrates under different conditions. The oxygen incorporated into the layer evaporated under poor vacuum is manifested as an additional step in the low energy region.

incorporated in the V layer is oxygen. Furthermore, this incorporation results in a reduced V density, as manifested by the lower height of the V peak from the layer evaporated in the poor vacuum. The rounding at the low energy edge of the V peak indicates an enhanced impurity incorporation at the start of evaporation, which produces a reduced V density over this region. From a knowledge of the measured [S] values from these composite layers and the oxygen and vanadium yields in the back-scattering spectra, absolute concentrations of both these elements can be calculated. Such a calculation is realized in the Appendix for the V layer whose spectrum is shown in Fig. 4.

Our interest in studying the variation of  $[S]$  values as a function of thickness and growth pressure stems from our studies of superconducting V layers with the back-scattering technique. A strong correlation has been found between variations in the superconducting transition temperature of this element and the  $[S]$  values. This dependence is shown in Fig. 5, where the superconducting transition temperature  $T_c$ , which has been found to be strongly dependent on impurity concentration, is shown as a function of pressure during evaporation. From a knowledge of such variations in  $[S]$  values with impurity incorporations, metal densities after layer growth can be determined and correlated, in our case, with superconducting properties.

In conclusion, it appears that FWHM measurements from back-scattering spectra coupled with an absolute determination of layer thickness offer a suitable technique for the evaluation of the back-scattering energy loss parameter  $[S]$ . Reasonable agreement has been found between the results obtained with this technique and  $[S]$  values calculated from the latest  $dE/dx$  values. The method, however, provides  $[S]$  values only for the geometry of one back-scattering system. Care has to be taken in  $[S]$  value determination from layers, since variation in layer properties may significantly influence the results obtained. Lower  $[S]$  values were found in this work for thin layer ( $< 500 \text{ \AA}$ ) growth and for layers where substantial impurity incorporation occurred. Correlation of these  $[S]$  values with other layer properties has also been observed.

ACKNOWLEDGEMENT

The authors are grateful to Mr. Ray Smithey for careful layer preparation and thickness measurements.

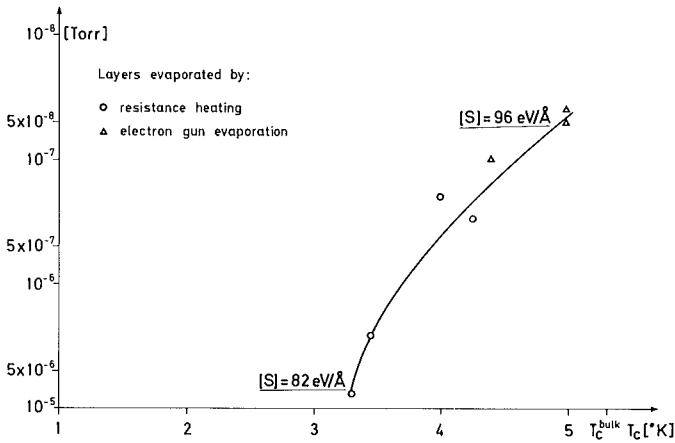


Fig. 5. The superconducting transition temperature  $T_c$  of V layers is plotted as a function of the vacuum used during layer preparation.  $[S]$  values determined for layers deposited in poor and good vacua are included.

## REFERENCES

- 1 J. W. Mayer, L. Eriksson and J. A. Davies, *Ion Implantation in Semiconductors*, Academic Press, New York, 1970, Ch. 3.
- 2 M. Croset, S. Rigo and G. Amsel, *Appl. Phys. Letters*, 19 (1971) 33.
- 3 O. Meyer, H. Mann and G. Linker, *Appl. Phys. Letters*, 20 (1972) 259.
- 4 J. F. Ziegler and W. K. Chu, *J. Appl. Phys.*, to be published; *IBM Rept RC 4288*.
- 5 O. Meyer, J. Gyulai and J. W. Mayer, *Surface Sci.*, 22 (1970) 263.
- 6 O. Meyer, G. Linker and B. Kraeft, *Thin Solid Films*, 19 (1973) 217.

## APPENDIX

*Calculation of absolute concentrations in  $V_xO_y$  from measured  $[S]$  values*

In the equations used in this appendix  $N$ ,  $R$  and  $[S]$  are, respectively, concentrations in atoms/cm<sup>3</sup>, back-scattering yields in counts and back-scattering energy loss parameters in eV/Å. The superscripts in the above parameters denote the scattering medium while the subscripts denote the atom for which the above parameters are determined.

In a compound with unknown composition (e.g.  $V_xO_y$ ) the concentration ratio  $Y$  of oxygen to vanadium atoms ( $= N_O^{V_xO_y}/N_V^{V_xO_y}$ ) can be calculated from <sup>6</sup>

$$Y = \frac{B_V}{B_O} \left( \frac{R_V^V}{R_V^{V_xO_y}} - 1 \right) \quad (A1)$$

with

$$B_V = \alpha_V (\varepsilon_V)_{E_1} + \frac{1}{\cos \theta_1} (\varepsilon_V)_{\alpha_V E_1}$$

$$B_O = \alpha_V (\varepsilon_O)_{E_1} + \frac{1}{\cos \theta_1} (\varepsilon_O)_{\alpha_V E_1}$$

where  $(\varepsilon_V)_{E_1}$ ,  $(\varepsilon_V)_{\alpha_V E_1}$  and  $(\varepsilon_O)_{E_1}$ ,  $(\varepsilon_O)_{\alpha_V E_1}$  are the stopping cross sections for vanadium and oxygen at energies  $E_1$  and  $\alpha E_1$  respectively. (Both  $\alpha$  and  $\theta$  ( $\theta_1 = 180 - \theta$ ) are defined in the main text.) From the measured  $[S]$  values and the known concentration in the bulk material, the absolute vanadium concentration  $N_V^{V_xO_y}$  in  $V_xO_y$  can be calculated from<sup>5</sup>

$$\frac{R_V^V}{R_V^{V_xO_y}} = \frac{N_V^V}{N_V^{V_xO_y}} \frac{[S_V^{V_xO_y}]}{[S_V^V]} \quad (A2)$$

and with the value of  $Y$  from eqn. (A1) the oxygen concentration  $N_O^{V_xO_y}$  in the vanadium oxide can be determined. Furthermore, eqn. (A2) can be modified to

$$\frac{R_V^V}{R_O^{V_xO_y}} = \frac{N_V^V}{N_O^{V_xO_y}} \frac{[S_O^{V_xO_y}]}{[S_V^V]} \frac{\sigma_V}{\sigma_O} \quad (A3)$$

where  $\sigma_V/\sigma_O$  is the ratio of Rutherford scattering cross sections for vanadium and oxygen; hence (since  $R_O^{V_xO_y}$  can be measured from the spectra)  $[S_O^{V_xO_y}]$  can be calculated. This  $[S]$  value can then be compared with that calculated using<sup>6</sup>

$$[S_{\text{O}}^{\text{V}_x\text{O}_y}] = \alpha_{\text{O}}(N_{\text{O}}^{\text{V}_x\text{O}_y} \varepsilon_{\text{O}} + N_{\text{V}}^{\text{V}_x\text{O}_y} \varepsilon_{\text{V}})_{E_1} + \frac{1}{\cos \theta_1} (N_{\text{O}}^{\text{V}_x\text{O}_y} \varepsilon_{\text{O}} + N_{\text{V}}^{\text{V}_x\text{O}_y} \varepsilon_{\text{V}})_{\alpha_{\text{O}} E_1} \quad (\text{A4})$$

an equation which infers the validity of Braggs' rule.

For the layer illustrated in Fig. 4 we find :

$$\begin{aligned} Y &= 0.38 & [S_{\text{O}}^{\text{V}_x\text{O}_y}]_{\text{exp}} &= 55 \text{ eV/\AA} \\ N_{\text{V}}^{\text{V}_x\text{O}_y} &= 4.74 \times 10^{22} \text{ V/cm}^3 \\ N_{\text{O}}^{\text{V}_x\text{O}_y} &= 1.82 \times 10^{22} \text{ O/cm}^3 & [S_{\text{O}}^{\text{V}_x\text{O}_y}]_{\text{cal}} &= 62 \text{ eV/\AA} \end{aligned}$$

The calculated and experimental  $[S]$  values for oxygen in  $\text{V}_x\text{O}_y$  are in good agreement within the experimental error, indicating the usefulness of the above procedure for  $[S]$  value determination in compounds. The results presented in this appendix demonstrate the capability of the back-scattering technique together with thickness measurements for determining both layer composition and atom concentrations.



## VALIDITY OF BRAGG'S RULE IN SPUTTERED SUPERCONDUCTING NbN AND NbC FILMS OF VARIOUS COMPOSITIONS\*

O. MEYER, G. LINKER AND B. KRAEFT

*Institut für Angewandte Kernphysik, Kernforschungszentrum, Karlsruhe (Germany)*

(Received August 10, 1973)

Niobium nitride layers have been produced by reactive sputtering in an argon-nitrogen plasma. Compositions were varied by altering the nitrogen partial pressure during the sputtering process. Changes in composition were determined by measuring the niobium peak height at the layer surface in back-scattered spectra, as well as by measuring the superconducting transition temperature  $T_c$  in homogeneous layers. These results are compared with niobium peak heights calculated as a function of the ratio of the number of nitrogen atoms to niobium atoms, using experimental and theoretical stopping cross sections for  $^4\text{He}^+$  ions in niobium and nitrogen. Assuming the validity of Bragg's rule in this calculation the measured values are found to be 7-8% smaller than those calculated. As uncertainties exist in present values of the stopping cross sections of Nb and N it is concluded that the observed deviation is too small to indicate whether or not Bragg's rule is applicable.

During the production of NbC layers in an Ar plasma the Nb target was covered by a perforated carbon plate. Stoichiometric layers have been produced with  $T_c$  values similar to that for bulk samples. The deviation between calculated and measured Nb peak heights is of the same order of magnitude as that found for NbN.

---

### INTRODUCTION

It has been shown<sup>1,2</sup> that reactively sputtered NbN films can be produced with superconducting properties superior to those of bulk samples. The highest transition temperature  $T_c$  reported for these films is  $17.3^\circ\text{K}$ <sup>1</sup>, which is about  $1^\circ$  higher than the highest value measured for bulk samples<sup>3</sup>. Although the critical field and critical current were found to be partially dependent upon film thickness and deposition temperature, the measured values were consistently higher for sputtered films than for bulk material<sup>4</sup>. For bulk samples it was found that the transition temperature is strongly dependent on the ratio of the number of nitrogen atoms to niobium atoms in the compound, the value of which is usually determined

---

\* Paper presented at the International Conference on Ion Beam Surface Layer Analysis, Yorktown Heights, New York, U.S.A., June 18-20, 1973.

by chemical analysis and lattice parameter measurements. As such measurements are difficult to perform on thin films, the sputtering parameters are usually optimized in order to obtain high  $T_c$  values.

In this study the back-scattering technique<sup>5</sup> was used to control and optimize the production of sputtered superconducting NbN and NbC films. In the analysis of the spectra produced by back-scattered high energy  $^4\text{He}^+$  ions, a knowledge of the electronic stopping power per target atom is of prime importance. From numerous measurements<sup>6-8</sup> of the specific energy loss for elemental materials, it is believed that the accuracy of the quoted values is of the order of  $\pm 5\%$ . For compounds, however, it is still uncertain whether Bragg's rule<sup>9</sup> on the linear superposition of the stopping cross sections for the different atoms is valid. In this respect the known dependence of  $T_c$  on the constituent atom ratio in superconducting interstitial compounds can be used to check the back-scattering results.

In this study we have therefore combined back-scattering and  $T_c$  measurements in order to check Bragg's rule for NbN and NbC.

#### EXPERIMENTAL

The vacuum system used in this study consisted of a bakable stainless-steel chamber connected to ion getter and titanium evaporation pumps. The background pressure prior to sputtering was usually of the order of  $10^{-8}$  torr. The cathode in this system was water cooled, whereas the temperature of the anode and the substrates was kept at  $450^\circ\text{C}$  before and during the sputtering process. The distance between anode and cathode was constant at 3 cm.

For NbN production, cleaned argon and nitrogen gas was used and while the partial pressure of argon was kept constant at  $10^{-2}$  torr the nitrogen pressure was varied in order to find optimum conditions for NbN formation. An a.c. power of 400 W was used so that the resulting current density was between 1 and  $1.3\text{ mA/cm}^2$ . Under these conditions the film growth rate was found to be about  $2\text{ \AA/sec}$ . Prior to deposition some of the Nb target was pre-sputtered onto a removable shield.

For NbC deposition, the Nb target was covered with a perforated carbon plate. The area ratio of C to Nb exposed to the plasma was varied between 0.5 and 0.2 in order to compensate for the different sputtering yields of the 2 keV argon ions on carbon and niobium. Both the NbN and NbC layers were deposited onto cleaned quartz and carbon substrates.

Transition temperature measurements were taken using a resistance method which employed a four-point probe arrangement situated in a helium cryostat.

Back-scattering measurements were performed using a beam of 2.0 MeV  $^4\text{He}^+$  ions from a Van de Graaff accelerator. Beam currents (typically 10 nA) were measured with a current integrator and secondary electrons were suppressed. Particles back-scattered through a laboratory angle of  $168^\circ$  were detected in a surface barrier detector and charge pulses generated were amplified and stored in a multichannel analyser. Dead time effects were avoided by the use of "fast" electronics and the system had an optimized resolution of 16 keV.

Thickness measurements of the NbN and NbC layers were performed with a

stylus instrument which measured the step height between the surface of the substrate and the surface of the deposited layer. The accuracy of this technique was usually limited by the surface flatness of the substrate and the deposited layers. In this study, layer thicknesses were measured to about  $\pm 50 \text{ \AA}$ .

## ANALYSIS

In Fig. 1 a typical back-scattering spectrum from a NbN layer sputtered onto a carbon substrate is compared with a spectrum from a Nb layer evaporated onto quartz. The height  $R_{\text{Nb}}^{\text{Nb}_x\text{N}_y}$  of the Nb peak in the  $\text{Nb}_x\text{N}_y$  layer is strongly reduced compared with the height  $R_{\text{Nb}}^{\text{Nb}}$  of the Nb peak in the evaporated Nb layer. This Nb peak yield was found to be comparable to yields from bulk Nb samples, suggesting a film density similar to that of bulk material.

The heights are given by the following equations<sup>9</sup>:

$$R_{\text{Nb}}^{\text{Nb}} = f N_{\text{Nb}}^{\text{Nb}} / [S_{\text{Nb}}^{\text{Nb}}] \quad (1a)$$

$$R_{\text{Nb}}^{\text{NbN}} = f N_{\text{Nb}}^{\text{NbN}} / [S_{\text{Nb}}^{\text{NbN}}] \quad (1b)$$

In the above equations  $f$  is a proportionality factor depending only on the geometry of the back-scattering experiment and the scattering cross section of niobium,  $N$  is the number of atoms and  $[S]$  is the back-scattering energy loss parameter.  $[S]$  is defined by

$$[S] = \alpha \left. \frac{dE}{dx} \right|_{E_0} + \frac{1}{\cos \theta_1} \left. \frac{dE}{dx} \right|_{\alpha E_0} \quad (2)$$

where  $\alpha$  is the fractional energy loss in the elastic collision,  $E_0$  is the energy of the incident  $^4\text{He}^+$  ion,  $\theta$  ( $= 180 - \theta_1$ ) is the laboratory back-scattering angle and

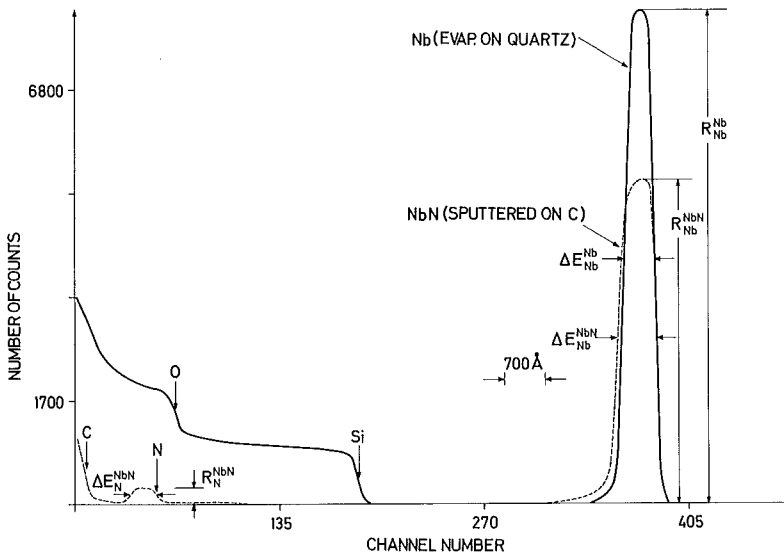


Fig. 1. Typical back-scattering spectra from a Nb layer evaporated onto a quartz substrate and from a NbN layer sputtered onto a carbon substrate.

$dE/dx$  is the specific energy loss at energies  $E_0$  and  $\alpha E_0$ . The superscripts in  $R$ ,  $N$  and  $[S]$  denote the scattering media and the subscripts denote the atom in the system causing the scattering. (Subscripts  $x$  and  $y$  in  $Nb_xN_y$  have been omitted for convenience.)

The specific energy loss  $dE/dx$  is defined as the product of the stopping cross section  $\varepsilon$  per atom and the density of the target atoms. Assuming that Bragg's rule of linear superposition of the stopping cross sections in a compound holds, we obtain for NbN:

$$\left. \frac{dE}{dx} \right|^{NbN} = \varepsilon_{Nb} N_{Nb}^{NbN} + \varepsilon_N N_N^{NbN} \quad (3)$$

Usually the physical properties of a compound, such as the transition temperature and the lattice parameter, are presented in terms of the constituent atom ratio  $Y$ , where

$$Y = N_N^{NbN} / N_{Nb}^{NbN}$$

Inserting eqns. (3) and (2) into eqns. (1a) and (1b) and using the ratio of (1b) to (1a), a simple relation is found between  $Y$  and the peak height  $R_{Nb}^{NbN}$  given by

$$Y = \frac{R_{Nb}^{Nb} B_{Nb}}{R_{Nb}^{NbN} B_N} - \frac{B_{Nb}}{B_N} \quad (4)$$

where

$$B_N = \alpha_{Nb} \varepsilon_{E_0}^N + \frac{1}{\cos \theta_1} \varepsilon_{\alpha E_0}^N$$

and

$$B_{Nb} = \alpha_{Nb} \varepsilon_{E_0}^{Nb} + \frac{1}{\cos \theta_1} \varepsilon_{\alpha E_0}^{Nb}$$

By inserting the theoretical and experimental values of stopping cross sections tabulated by Ziegler and Chu<sup>8</sup> into eqn. (4) and using an experimentally determined value for  $R_{Nb}^{Nb}$ , we obtain the values presented in Fig. 2. The calculations have been performed only for a narrow region of  $Y$ , *i.e.*  $0.75 < Y < 1.1$ , but it is in this region that the superconducting  $\delta$ -phase of NbN exists. Included in Fig. 2 are the calculated values for NbC using theoretical stopping cross sections.

In an interstitial compound of the NaCl type such as NbN, the dependence of atom density on  $Y$  may be discussed in terms of two models. In model A, the model of closest packing, it is assumed that the total number of atoms is constant. The atom densities for this model are thus

$$N_{Nb}^{NbN} = \frac{100-Z}{100} N_{Nb, N} \quad \text{and} \quad N_N^{NbN} = \frac{Z}{100} N_{Nb, N}$$

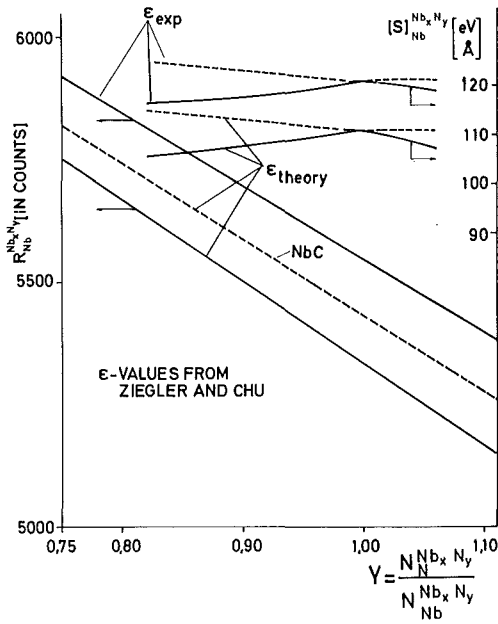


Fig. 2. Calculated values of the niobium peak height at the surface and the  $[S]$  values, showing their dependence on the composition. In both calculations theoretical and experimental stopping cross sections from Ziegler and Chu were used.

where  $Z$  is the number of N atoms in percent and  $N_{\text{Nb}, \text{N}} = 8/a^3$  atoms/cm<sup>3</sup> is the total number of atoms ( $a$  is the lattice parameter). Here we find

$$\left. \frac{dE}{dx} \right|^{NbN} = \frac{8}{a^3(1+Y)} (\epsilon_{\text{Nb}} + Y\epsilon_{\text{N}}) \quad (5)$$

In model B it is assumed that for  $Y < 1$  there are nitrogen vacancies but the number of niobium atoms is constant and equal to  $4/a^3$ . For  $Y > 1$  the number of nitrogen atoms is equal to  $4/a^3$  and niobium vacancies exist. For this model we obtain

$$\left. \frac{dE}{dx} \right|^{NbN} = \frac{4}{a^3} (\epsilon_{\text{Nb}} + \epsilon_{\text{N}} Y) \quad \text{for } Y < 1$$

$$\left. \frac{dE}{dx} \right|^{NbN} = \frac{4}{a^3} \left( \frac{1}{Y} \epsilon_{\text{Nb}} + \epsilon_{\text{N}} \right) \quad \text{for } Y > 1 \quad (6)$$

Model B is generally thought to be the correct one as it has been found<sup>10</sup> that the lattice parameter has a shallow maximum at  $Y = 1$ . The calculated dependences of  $[S]$  on  $Y$  for both models, using the theoretical and experimental values of stopping cross sections<sup>8</sup>, are included in Fig. 2. In these calculations the changes in lattice parameter, which are less than 1%, have been considered. The results show that careful thickness measurements are necessary in order to obtain accurate  $[S]$  values from the equation  $\Delta E = t[S]$ , where  $\Delta E$  is the full width at half maximum, as indicated in Fig. 1.

## RESULTS AND DISCUSSION

The influence of the nitrogen partial pressure on  $R_{\text{Nb}}^{\text{NbN}}$  during the formation of NbN layers is demonstrated in Fig. 3. The back-scattering spectrum, shown as a solid line, was obtained from a sample for which nitrogen was introduced for two short periods during deposition. The fluctuations in the Nb peak height indicate the regions of nitride formation; this formation stops when the nitrogen gas is consumed. The second spectrum (broken line) was obtained from a sample where constant nitrogen flows were used at partial pressures of  $1.7 \times 10^{-2}$  torr and  $10^{-3}$  torr. This spectrum shows clearly that for the formation of NbN in our equipment the partial pressure of nitrogen has to be higher than  $10^{-3}$  torr. This result is in contrast to results presented in ref. 1 where an optimum nitrogen partial pressure of  $10^{-4}$  torr was reported. It is suggested that this discrepancy may be due to differences in partial pressure measurements. The height of the Nb peak at the layer surface has been determined for  $\text{Nb}_x\text{N}_y$  layers produced under a constant flow of nitrogen and in Fig. 4 the dependence of the peak height on nitrogen partial pressure is demonstrated. In the pressure range between  $10^{-2}$  and  $4 \times 10^{-2}$  torr there is only a 7% change in the Nb peak height, whereas between  $4 \times 10^{-3}$  and  $5 \times 10^{-3}$  torr the peak height increases markedly.

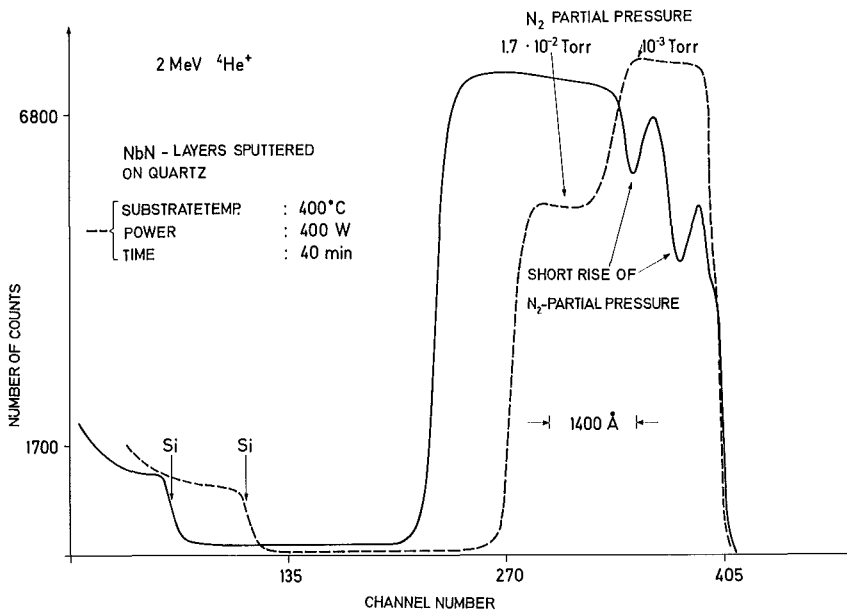


Fig. 3. Back-scattering spectra from sputtered NbN layers. The effect of altering the nitrogen partial pressure during the sputtering process is clearly demonstrated.

For niobium carbides and nitrides, Horn and Saur<sup>3</sup> and Geballe *et al.*<sup>11</sup> found that the superconducting transition temperature depends strongly on composition. Their results obtained by chemical analysis and lattice parameter measurements on bulk probes are shown in Fig. 5, together with measured  $T_c$ .

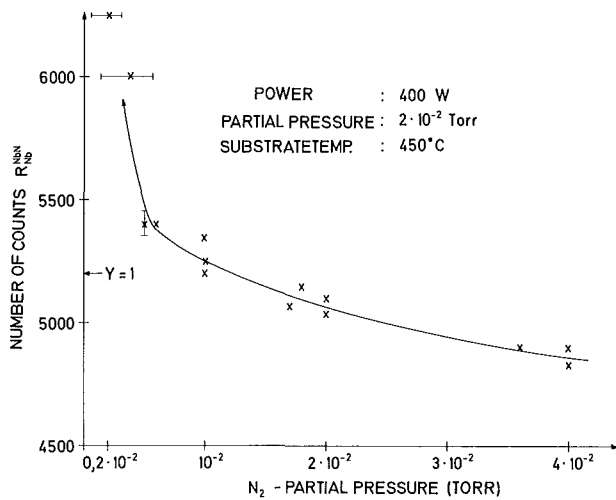


Fig. 4. Nitrogen partial pressure vs. niobium peak height at the surface.

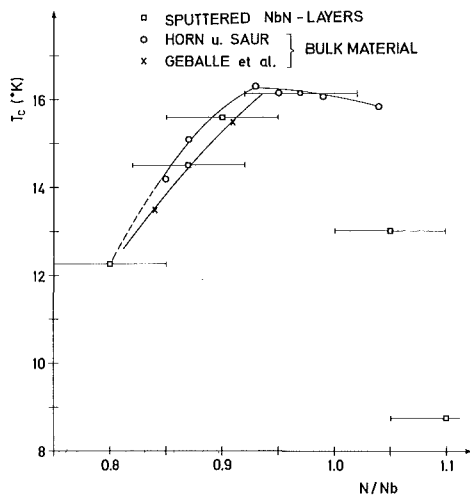


Fig. 5. Dependence of the superconducting transition temperature on composition for NbN bulk samples and for sputtered NbN layers.

values for thin sputtered NbN films. During  $T_c$  measurements on thin NbN and NbC layers two difficulties should be stressed.

(a) For films with thicknesses less than  $500 \text{ \AA}$ ,  $T_c$  is strongly suppressed. This may be partly due to impurity incorporation during the first growth stages.

(b) Using resistance measurements for  $T_c$  determination a high  $T_c$  value may be obtained even if only part of the layer has the correct composition. Therefore only those films were considered which, from analysis with the back-scattering technique, appeared to be homogeneous. The measured  $T_c$  values for those charges (one charge consisted usually of five samples) that fulfilled this condition are presented in Fig. 5.

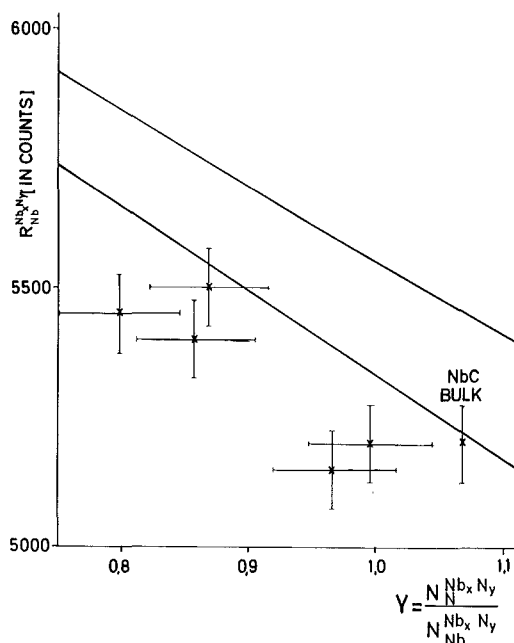


Fig. 6. Measured niobium peak heights of sputtered NbN layers *vs.* composition. The calculated dependence from Fig. 2 is included for comparison.

The measured Nb peak heights and the corresponding composition values, determined from Fig. 5 in the region where the superconducting  $\delta$ -phase exists, are presented in Fig. 6. The niobium peak height dependence on  $Y$  could be further verified by measuring bulk samples of NbN and NbC of known composition and by measuring, from the back-scattering spectrum, the peak area ratios  $A_N/A_{Nb}$  of thin NbN films with high  $T_c$  values. In general the measured values follow the dependence of  $Y$  on  $R_{Nb}^{NbN}$  calculated from eqn. (4).

Assuming that the experimental values for the stopping cross sections are more accurate than the theoretical values,  $(dE/dx)^{NbN}$  has been evaluated from Bragg's rule using these experimental stopping cross sections. Calculated Nb peak heights from the  $(dE/dx)^{NbN}$  results led to values 7–8% higher than those measured in the back-scattered NbN spectra. As the  $\epsilon$  values for niobium have not yet been measured directly to our knowledge but have been extrapolated from measured values for Mo, some reservations must be made in the assumption that Bragg's rule does not apply. Also our first results for  $[S_{Nb}^{Nb}]$  obtained from thin Nb films are still uncertain because of problems due to impurity incorporation during film deposition<sup>1,2</sup>. Further work is currently being conducted in an attempt to clarify the issue.

The main difficulties involved with the production of sputtered NbC films were due to the inhomogeneous distribution of atoms through the films. This is demonstrated in Fig. 7 by spectra obtained from samples produced under different target arrangements. A spectrum from an evaporated Nb layer is included here for comparison, together with a spectrum for a stoichiometric NbC bulk sample.

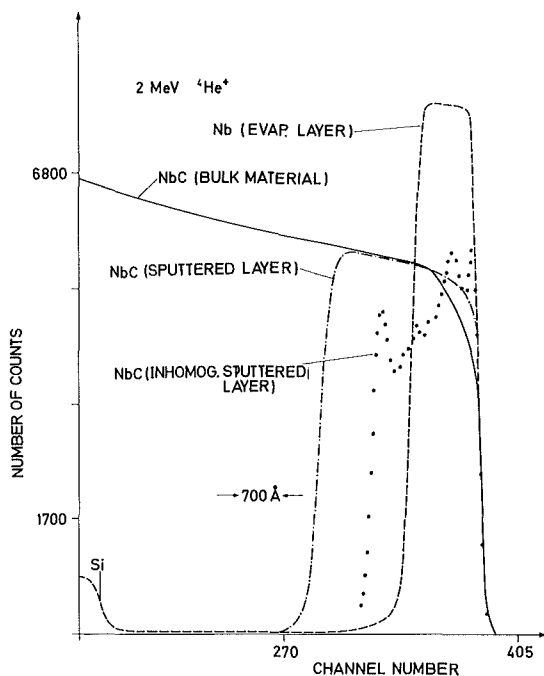


Fig. 7. Back-scattering spectra from an evaporated Nb layer, a stoichiometric NbC bulk sample, and from an inhomogeneous and a homogeneous NbC layer sputtered onto quartz substrates.

The use of a perforated carbon sheet resulted in the production of highly inhomogeneous layers, as indicated by the points in Fig. 7. These inhomogeneities were thought to be due to plasma instabilities near the sharp edges of the holes in the carbon. Smoothing of these edges resulted in more homogeneous layers (chain curve in Fig. 7) which had critical temperatures of  $11.5^{\circ}\text{K}$ , the highest  $T_c$  value which has been reported for bulk NbC. Although we have made sputtered NbC layers with high  $T_c$  values (to our knowledge this is the first time that such layers have been achieved) it was found to be very difficult to change the composition while at the same time keeping a homogeneous layer. This difficulty has prevented us from studying Nb peak heights as a function of composition in niobium carbides. A value found for stoichiometric samples, however, has been included in Fig. 6, where again the agreement with the calculated peak height value from Fig. 2 is considered to be good.

In conclusion, it can be said that back-scattering analysis proves to be a useful technique in the study of formation processes of sputtered superconducting layers. It is especially useful when a sputter target such as a high purity compound is not available and therefore a non-continuous target material arrangement has to be used. The inhomogeneities in such layers can easily be monitored both in depth and laterally and optimum growth conditions can be found. The sharp variation in  $T_c$  with composition, in the region of the existence of the superconducting  $\delta$ -phase, can be used with advantage as an independent check of the  $Y$  dependence on the niobium peak height as given by eqn. (4). For the analysis

of the composition and the impurity content of thin film compounds with an accuracy to better than 5%, there is still an increasing need to know the energy loss of  $^4\text{He}^+$  ions in matter with greater precision. It is this lack of precision which prevents us from stating whether or not Bragg's rule is applicable to the compound niobium nitride.

#### ACKNOWLEDGEMENTS

We gratefully acknowledge the assistance of Mr. F. Ratzel who performed the sputtering experiments. We also wish to thank Dr. M. Gettings for valuable discussions.

#### REFERENCES

- 1 J. R. Gavaler, J. K. Hulm, M. A. Janocko and C. K. Jones, *J. Vac. Sci. Technol.*, 6 (1969) 177.
- 2 Y. Saito, T. Anayama, Y. Onodera, T. Yamashita, K. Konenon and Y. Muto, *Proc. 12th Intern. Conf. on Low Temperature Physics, Kyoto, Japan, Sept. 1970*, p. 329.
- 3 G. Horn and E. Saur, *Z. Physik*, 210 (1968) 70-79.
- 4 J. K. Hulm, J. R. Gavaler, M. A. Janocko, A. Patterson and C. K. Jones, *Proc. 12th Intern. Conf. on Low Temperature Physics, Kyoto, Japan, Sept. 1970*, p. 325.
- 5 M.-A. Nicolet, J. W. Mayer and I. V. Mitchell, *Science (N.Y.)*, 177 (1972) 841-849.
- 6 W. Whaling, in S. Flügge (ed.), *Handbuch der Physik*, Vol. 34, Springer, Berlin, 1958.
- 7 W. K. Chu and D. Powers, *Phys. Rev.*, 187 (1969) 187.
- 8 J. F. Ziegler and W. K. Chu, *IBM Research RC 4288*, March 29, 1973.
- 9 O. Meyer, J. Gyulai and J. W. Mayer, *Surface Sci.*, 22 (1970) 263.
- 10 G. Brauer and H. Kirner, *Z. Anorg. Allgem. Chem.*, 328 (1964) 34.
- 11 T. H. Geballe, B. T. Matthias, J. P. Remeika, A. M. Clogston, V. B. Compton, J. P. Maita and H. J. Williams, *Physics*, 2 (1966) 293.
- 12 G. Linker, O. Meyer and M. Gettings, *Thin Solid Films*, 19 (1973) 177.